Applied Mathematical Modelling 75 (2019) 806–818

Contents lists available at ScienceDirect

Applied Mathematical Modelling

journal homepage: www.elsevier.com/locate/apm

Suppression of epidemic spreading in time-varying multiplex networks

Hui Yang[b,c], Changgui Gu[d], Ming Tang[a,e,*], Shi-Min Cai[c,f], Ying-Cheng Lai[g]

[a] Shanghai Key Laboratory of Pure Mathematics and Mathematical Practice, School of Mathematical Sciences, East China Normal University, Shanghai 200241, China
[b] Cyberspace Security Key Laboratory, China Electronics Technology Group Corporation, Chengdu, China
[c] Web Sciences Center, University of Electronic Science and Technology of China, Chengdu 611731, China
[d] Business School, University of Shanghai for Science and Technology, Shanghai, China
[e] Shanghai Key Laboratory of Multidimensional Information Processing, East China Normal University, Shanghai 200241, China
[f] Big Data Research Center, University of Electronic Science and Technology of China, Chengdu 611731, China
[g] Department of Electrical Engineering, Arizona State University, Tempe, AZ 85287, USA

ARTICLE INFO

Article history:
Received 9 January 2019
Revised 27 May 2019
Accepted 2 July 2019
Available online 5 July 2019

Keywords:
Multiplex network
Time-varying
Epidemic spreading
Microscopic Markov chain

ABSTRACT

Suppressing and preventing epidemic spreading is of critical importance to the well being of the human society. To uncover phenomena that can guide control and management of epidemics is thus of significant value. An understanding of epidemic spreading dynamics in the real world requires the following two ingredients. Firstly, a multiplex network description is necessary, because information diffusion in the virtual communication layer of the individuals can affect the disease spreading dynamics in the physical contact layer, and vice versa. The interaction between the dynamical processes in the two layers is typically asymmetric. Secondly, both network layers are in general time varying. In spite of the large body of literature on spreading dynamics in complex networks, the effect of the asymmetrical interaction between information diffusion and epidemic spreading in activity-driven, time-varying multiplex networks have not been understood. We address this problem by developing a general theory based on the approach of microscopic Markov chain, which enables us to predict the epidemic threshold and the final infection density in the physical layer, on which the information diffusion process in the virtual layer can have a significant effect. The focus of our study is on uncovering and understanding mechanisms to inhibit physical disease spreading. We find that stronger heterogeneity in the individual activities and a smaller contact capacity in the communication layer can promote the inhibitory effect. A remarkable phenomenon is that an enhanced positive correlation between the activities in the two layers can greatly suppress the spreading dynamics, suggesting a practical and effective approach to controlling epidemics in the real world.

1. Introduction

Epidemic outbreaks are a major threat to the human society [1–5], rendering critically important to devise effective control and mitigation strategies. Because of the infeasibility to conduct actual experiments, mathematical modeling and

* Corresponding author at: Shanghai Key Laboratory of Pure Mathematics and Mathematical Practice, School of Mathematical Sciences, East China Normal University, Shanghai 200241, China.
E-mail address: tangminghan007@gmail.com (M. Tang).

https://doi.org/10.1016/j.apm.2019.07.011
0307-904X/

analysis have become an indispensable tool to understand, predict and devise strategies to control and manage the dynamics of epidemic spreading. In this regards, not only should the underlying model be analyzable, it is also imperative that realistic factors are incorporated into the model. For any modeling effort, a key goal is to identify the mechanisms and phenomena that can be exploited for controlling and managing epidemic spreading to prevent large scale outbreaks. These general considerations have motivated the present work. In particular, we construct and analyze a time-varying multiplex network model for spreading dynamics, taking into account real-world factors such as the asymmetric inter-network layer interactions. A key finding of this work with significant implications to control and management is that enhancing the positive correlation between the activities in the virtual communication and physical contact layers can greatly suppress the spreading dynamics.

The study of spreading dynamics has a long history. Early on, a number of paradigmatic models, such as the susceptible-infected (SI), susceptible-infected-recovered (SIR), and susceptible-infected-susceptible (SIS) models were proposed [6]. The development of complex network science about two decades ago has stimulated a great deal of work on uncovering the effects of network structure on epidemic spreading [7–9]. A key quantity of interest is the epidemic threshold, the critical value of a parameter (e.g., some kind of transmission rate) at which an outbreak of the disease occurs. A seminal contribution to this field was the discovery that the epidemic threshold in networks with a heterogeneous degree distribution can be vanishingly small in the thermodynamic limit [7,9].

A realistic factor that ought to be taken into account in studying epidemic spreading dynamics is the multilayer structure of the underlying networked system. In particular, as an epidemic breaks out, information about the disease can spread, leading to the emergence of crisis awareness among the individuals in the population [10–12]. As a natural response, certain individuals would take preventive measures to protect themselves from the disease [13], such as wearing a mask, paying particular attention to personal hygiene, avoiding contacts with potential sources of infection, and enhancing their immune system through medicine and/or physical exercises. The underlying complex networked system supporting the spreading dynamics thus possesses at least two layers with the identical set of nodes: the physical contact layer and the virtual layer of information diffusion. The dynamical process in the virtual layer can impact significantly the spreading dynamics in the physical layer, e.g., a reduction in the effective infectivity of the disease, a shortened duration of the disease for those who are infected, and a decreased level of susceptibility of the aware individuals to the disease, and so on. It was demonstrated quantitatively that information-based behavior response can indeed mitigate epidemic outbreaks [14–18] in that the size of the outbreak is reduced and the outbreak threshold is raised. The potential impacts on the spreading dynamics in the physical contact network depend on the type of the diffused information in the virtual network. For example, global information about the prevalence of the disease in general is not helpful for reducing the likelihood of epidemic outbreak, while local information, such as the density of infected individuals in a small neighborhood, can serve to suppress the outbreak [19,20]. Driven by information spreading, voluntary vaccination can spontaneously arise, in addition to compulsory immunization as stipulated by governmental organizations [21].

Disease spreads through the physical contact network formed by daily interactions among the individuals, while information exchanges on the virtual contact layer occur through some kind of communication systems such as online social networks, instant communication tools, and various news media. The underlying multiplex, contact-communication coupled network thus constitutes layers with different types of interaction [22–26]. A realistic feature of multiplex networks is that the interactions between the two layers are not symmetric. In fact, the effect of one layer on another can be opposite when the direction of the interaction is reversed. In this regard, previous studies of an asymmetrically interacting spreading model on multiplex networks revealed that epidemic spreading in the physical contact layer can boost information spreading in the virtual layer, while information spreading can inhibit the physical spreading process [27–29]. The existence of a metacritical point was uncovered, from which the critical onset of the epidemic tends to depend on the completion of the information spreading process [28,29]. It was also found that, when the effects of mass media are taken into account, the metacritical point disappears [30], indicating that its emergence can be attributed to the complex interplay between epidemic and information dynamics. Similar results were obtained from a model that incorporates information-driven vaccination adoption and hosts a complex non-Markovian process [31]. It was also found that a link similarity between the two network layers determines the likelihood of inhibiting the infection when the precaution level is sufficiently high [32]. In these previous studies, the multiplex networked systems were assumed to be static.

In reality, both the physical contact and the information diffusion layers are not static but time varying. Static connections and interactions are approximate in the sense that they are the time-aggregated representation of the actual interactions, with the time-varying nature of the connectivity patterns completely ignored. For a more accurate understanding of epidemic spreading dynamics in the real world, time-dependent interactions between the network layers need to be taken into account. At the present, in the field of epidemic spreading, there are two types of time dependent systems: adaptive networks [33–36] and temporal networks [37–39], where the former emphasize the response of the network structure to the dynamics on it, while the latter focus on the timing validity of the interaction events.

To be concrete, in this paper we focus on a class of temporal networks, the activity-driven networks [38]. Recent studies have demonstrated that temporal variations are important in many social systems [40–42] and the diffusive processes in temporal networks are different from those in the corresponding static, time-aggregated networks [38,39]. These efforts have made it possible to address an issue that was poorly understood: how temporal variations affect the asymmetrically interacting dynamics between disease spreading and information diffusion. To accomplish this, we first introduce a class of two-layer, activity driven networks (Section 2). We then develop a microscopic Markov chain (MMC) approach to analyzing

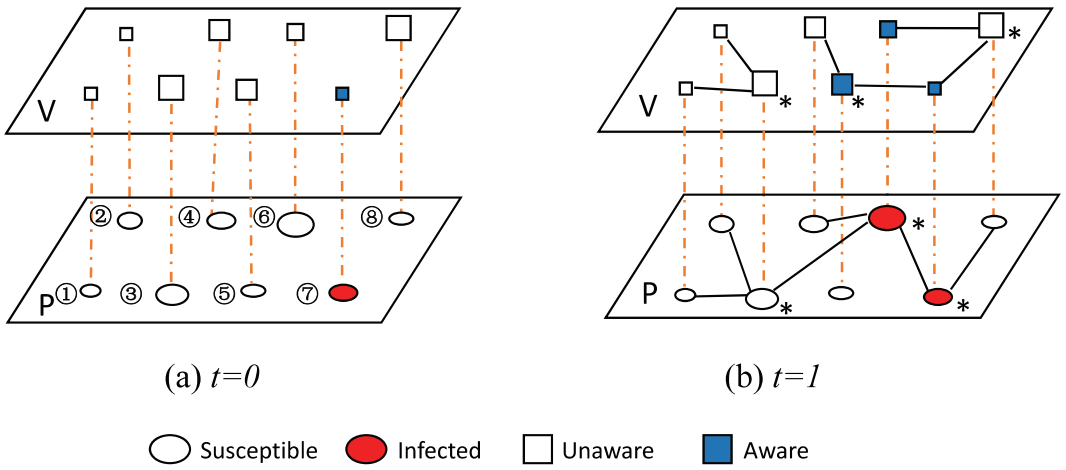

Fig. 1. Model illustration: asymmetrically interacting spreading in a time varying network with two layers. The physical contact and virtual communication layers are denoted as $\mathcal{P}$ and $\mathcal{V}$, respectively. There is a one-to-one nodal correspondence between $\mathcal{P}$ and $\mathcal{V}$, where each pair of the corresponding nodes is assigned the same index in both layers. The size of an ellipse or a square represents the activity level of the node, where a larger size indicates a higher level of nodal activity. (a) At $t = 0$, there are N isolated nodes with different activity levels in the two layers and node 7 is randomly chosen as the infected seed in $\mathcal{P}$, so that it is in the state of being aware in $\mathcal{V}$. The remaining nodes are in the *US* state, i.e., being susceptible in $\mathcal{P}$ and unaware in $\mathcal{V}$. (b) At $t = 1$, an instantaneous network is generated according to the nodal activities, where nodes 3, 6 and 7 in $\mathcal{P}$ and nodes 3, 5 and 8 in $\mathcal{V}$ are activated, which are marked with an asterisk in the lower right corner of each node. Each active node generates m links that are connected to randomly chosen nodes. For example, node 5 gets informed by node 7 in $\mathcal{V}$ with the probability $\lambda\Delta t$, where $\Delta t = 1$. Node 6 is infected by node 7 in $\mathcal{P}$ with the probability $\beta\Delta t$ and so is informed in $\mathcal{V}$. At the next time step, all the links are removed and the processes at $t = 1$ are repeated. This continues until the spreading dynamics in both layers have terminated or have reached a stationary state.

the asymmetric spreading dynamics, which allows us to predict the epidemic threshold and the final infection density (Section 3). Comparing the MMC predictions with results from direct simulations (Section 4), we find that time dependence can induce inhibition of the spreading dynamics by information diffusion. A result is that stronger heterogeneity in the individual activities and a smaller contact capacity in the virtual communication layer can enhance the inhibition. The main phenomenon uncovered is that an enhanced correlation between the activities in the two layers can greatly suppress the spreading dynamics, providing the base for informing policies to control and manage epidemics in the real world.

2. Asymmetrically interacting spreading model in time-varying multiplex networks

To construct a general model for asymmetrically interacting spreading dynamics in time-varying networks, we begin by defining an activity-driven duplex network. The network is composed of a physical contact layer $\mathcal{P}$ and a virtual communication layer $\mathcal{V}$, where the structures of both layers depend on time. Each layer is generated by an activity-driven generative algorithm [38]. There are N nodes in the network and each node is of a fixed individual activity level. The activity level of a node is defined as the probability that the node activates itself and creates new interacting links with other nodes at each time step, in either physical contact layer or virtual communication layer. The activity levels of node i are set respectively as $a_i = \eta_v x_i$ in layer $\mathcal{V}$ and $b_i = \eta_p y_i$ in layer $\mathcal{P}$, where η_v and η_p are the respective rescaling factors. The activity potentials x_i and y_i respectively obey the power-law distributions $F_v(x) \propto x^{-\gamma_v}$ and $F_p(y) \propto y^{-\gamma_p}$, and are bounded as $\epsilon \le x_i \le 1$ and $\epsilon \le y_i \le 1$ where ϵ is a lower cut-off (we set $\epsilon = 10^{-3}$). Parameters γ_v and γ_p are called as activity exponents of layers V and P, respectively. A smaller value of activity exponent γ_v or γ_p gives a more heterogeneous activity distribution in the corresponding layer.

Fig. 1 illustrates the three steps in the construction of the time-varying virtual (physical) layer, which are described as follows. Firstly, at each time step t, the network of each layer consists of N disconnected nodes, and there is a one-to-one correspondence between nodes in the two layers. Secondly, with probability $a_i\Delta t$ ($b_i\Delta t$), node i becomes active and generates m_v (m_p) links to randomly selected nodes, for $i = 1, \ldots, N$. Thirdly, for the next time step, all links are removed and the processes in the first and second steps are repeated until the spreading dynamics in both layers are terminated or reach a stationary state. At each time step, the mean degrees of layers $\mathcal{V}$ and $\mathcal{P}$ are $\langle k_v\rangle = 2m_v\langle a\rangle = 2m_v\eta_v\langle x\rangle$ and $\langle k_p\rangle = 2m_p\langle b\rangle = 2m_p\eta_p\langle y\rangle$, respectively. For specific values of the exponent γ_v (γ_p) and m_v (m_p), by changing the value of η_v or η_p, we can get a snapshot of the network with the specific value of the mean degree $\langle k_v\rangle$ or $\langle k_p\rangle$.

The next step is to define the disease-information asymmetrical interacting spreading model. The information spreading process in $\mathcal{V}$ is described by the unaware-aware-unaware (UAU) type of dynamics, where a node can be either in an aware (of the disease) or an unaware state, denoted by A and U, respectively. In the physical contact layer $\mathcal{P}$, the conventional SIS process takes place, where any node can be susceptible (S) or infected (I). A node in the whole duplex network can then be in three distinct states: unaware and susceptible (*US*), aware and susceptible (*AS*), and aware and infected (*AI*), as illustrated in Fig. 1. In our model, unaware nodes get information and become aware from each A neighbor at the information

Table 1
Description of symbols.

Symbol	Description
N	Number of nodes in network
t	Time step
m_v	The number of links the active nodes in layer $\mathcal{V}$ generate in a time step
m_p	The number of links the active nodes in layer $\mathcal{P}$ generate in a time step
a_i	Activity level of node i in layer $\mathcal{V}$
b_i	Activity level of node i in layer $\mathcal{P}$
η_v	Rescaling factor in layer $\mathcal{V}$
η_p	Rescaling factor in layer $\mathcal{P}$
x_i	Activity potential of node i in layer $\mathcal{V}$
y_i	Activity potential of node i in layer $\mathcal{P}$
$F_v(x)$	The distribution of node's activity potential in layer $\mathcal{V}$
$F_p(y)$	The distribution of node's activity potential in layer $\mathcal{P}$
ϵ	A lower cut-off of activity potential distribution
γ_v	Activity exponent of layer $\mathcal{V}$
γ_p	Activity exponent of layer $\mathcal{P}$
$\langle k_v \rangle$	Mean degree of layer $\mathcal{V}$
$\langle k_p \rangle$	Mean degree of layer $\mathcal{P}$
λ	Information transmission rate
δ	Information recovery rate
β	Disease transmission rate
μ	Disease recovery rate
β^U	Disease transmission rate for U node
β^A	Disease transmission rate for A node
κ	A factor to capture the difference between β^U and β^A: $\beta^A = \kappa\beta^U$
P_i^X	The probability that node i is in state X
$r_i(t)$	The probability that node i is not informed by any neighbor at time t
$q_i^A(t)$	The probabilities of an A node not being infected by any neighbor at time t
$q_i^U(t)$	The probabilities of a U node not being infected by any neighbor at time t

transmission rate λ. At the same time, a node, once in the A state, forgets or does not care about the information any longer and returns to the U state at the recovery rate δ. The disease propagates from an infected node to each of its susceptible neighbors with disease transmission rate β and each infected node recovers to the susceptible state at the rate μ. If a node is in the I state in $\mathcal{P}$, it will automatically be aware of the information and thus in the aware state in $\mathcal{V}$. Let β^U and β^A be the disease transmission rates for the U and A nodes, respectively. Nodes simultaneously in the A state in $\mathcal{V}$ and in the S state in $\mathcal{P}$ are likely to take measures to protect themselves from being infected. As a result, if a node is aware and susceptible, the disease transmission rate will be reduced by a factor κ: $\beta^A = \kappa\beta^U$, where $\beta^U = \beta$. For simplicity, we assume that the A nodes are completely immune to the disease by setting $\kappa = 0$.

3. Microscopic Markov chain approach

Let us denote the probability that node i is in state X as P_i^X, where $X \in \{U, A, S, I, US, AS, AI\}$. For node i with activity levels a_i and b_i in $\mathcal{V}$ and $\mathcal{P}$, respectively, the probability that this node is not informed by any neighbor at time t is

$$r_i(t) = \prod_j \left[1 - \lambda \frac{m_v}{N}(a_i P_j^A(t) + a_j P_j^A(t))\right], \tag{1}$$

where $P_j^A(t) = P_j^{AI}(t) + P_j^{AS}(t)$. The term $\frac{m_v}{N}(a_i P_j^A(t) + a_j P_j^A(t))$ on the right-hand side of Eq. (1) is the probability that node j is node i's A neighbor, where the first part $\frac{m_v}{N} a_i P_j^A(t)$ is the probability that active node i creates a link with A node j and the second part $\frac{m_v}{N} a_j P_j^A(t)$ is the probability that node i gets a link from active A node j. Similarly, the probabilities of an A node and of a U node not being infected by any neighbor at time t are, respectively,

$$q_i^A(t) = \prod_j \left[1 - \beta^A \frac{m_p}{N}(b_i P_j^{AI}(t) + b_j P_j^{AI}(t))\right], \tag{2}$$

$$q_i^U(t) = \prod_j \left[1 - \beta^U \frac{m_p}{N}(b_i P_j^{AI}(t) + b_j P_j^{AI}(t))\right], \tag{3}$$

where the terms $\frac{m_p}{N}(b_i P_j^{AI}(t) + b_j P_j^{AI}(t))$ and $\frac{m_p}{N}(b_i P_j^{AI}(t) + b_j P_j^{AI}(t))$ on the right hand side of the two equations are the respective probability that node j is node i's infected neighbor. Description of all symbols are listed in Table 1.

The characteristics of the asymmetrically interacting spreading dynamics on the two network layers [28] suggest that the approach of microscopic Markov chains be exploited for theoretical analysis and prediction. In particular, the transition

probabilities for the coupled process between node i with activity levels a_i and b_i in $\mathcal{V}$ and $\mathcal{P}$, respectively, can be written as

$$P_i^{US}(t+1) = P_i^{AI}(t)\delta\mu + P_i^{US}(t)r_i(t)q_i^U(t) + P_i^{AS}(t)\delta q_i^U(t), \tag{4}$$

$$P_i^{AS}(t+1) = P_i^{AI}(t)(1-\delta)\mu + P_i^{US}(t)[1-r_i(t)]q_i^A(t) + P_i^{AS}(t)(1-\delta)q_i^A(t), \tag{5}$$

$$\begin{aligned} P_i^{AI}(t+1) = {} & P_i^{AI}(t)(1-\mu) + P_i^{US}(t)\{[1-r_i(t)][1-q_i^A(t)] \\ & + r_i(t)[1-q_i^U(t)]\} + P_i^{AS}(t)\{\delta[1-q_i^U(t)] + (1-\delta)[1-q_i^A(t)]\}. \end{aligned} \tag{6}$$

The stationary solutions of the system can be obtained as a set of fixed points satisfying the relations

$$\begin{aligned} &P_i^{AI}(t+1) = P_i^{AI}(t) = P_i^{AI}, \\ &P_i^{AS}(t+1) = P_i^{AS}(t) = P_i^{AS}, \text{ and} \\ &P_i^{US}(t+1) = P_i^{US}(t) = P_i^{US}. \end{aligned}$$

At the onset of epidemic spreading, the probability of nodes to be infected in layer $\mathcal{P}$ is negligible, i.e., $P_i^{AI} \ll 1$. Eq. (2) can be approximated as

$$\begin{aligned} q_i^A &\approx 1 - \sum_j \beta^A \frac{m_p}{N}(b_i P_j^{AI} + b_j P_j^{AI}) \\ &= 1 - m_p\beta^A(b_i\rho^{AI} + \theta_b^{AI}), \end{aligned} \tag{7}$$

where

$$\rho^{AI} = \frac{1}{N}\sum_{j=1}^{N} P_j^{AI},$$

$$\theta_b^{AI} = \frac{1}{N}\sum_{j=1}^{N} b_j P_j^{AI}.$$

Similarly, Eq. (3) can be approximated as

$$q_i^U \approx 1 - m_p\beta^U(b_i\rho^{AI} + \theta_b^{AI}). \tag{8}$$

Using these conditions, we can simplify the stationary solution equations of Eqs. (4)–(6) as

$$P_i^{US} = P_i^{US}r_i + P_i^{AS}\delta, \tag{9}$$

$$P_i^{AS} = P_i^{US}(1-r_i) + P_i^{AS}(1-\delta), \tag{10}$$

$$\mu P_i^{AI} = P_i^{US}[(1-r_i)(1-q_i^A) + r_i(1-q_i^U)] + P_i^{AS}[\delta(1-q_i^U) + (1-\delta)(1-q_i^A)]. \tag{11}$$

Eq. (11) can be further approximated as

$$\begin{aligned} \mu P_i^{AI} &= P_i^{AS}(1-q_i^A) + P_i^{US}(1-q_i^U) \\ &\approx m_p\beta(b_i\rho^{AI} + \theta_b^{AI})[1-(1-\kappa)P_i^A]. \end{aligned} \tag{12}$$

Taking average over all nodes, we get the proportion of the infected nodes in the system as

$$\mu\rho^{AI} = \mu\frac{1}{N}\sum_{i=1}^{N} P_i^{AI},$$

which can be simplified as

$$\mu\rho^{AI} = m_p\beta\{\rho^{AI}[\langle b\rangle - (1-\kappa)\theta_b^A] + \theta_b^{AI}[1-(1-\kappa)\rho^A]\}, \tag{13}$$

where $\rho^A = (1/N)\sum_{j=1}^{N} P_j^A$ and $\theta_b^A = (1/N)\sum_{j=1}^{N} b_j P_j^A$. Multiplying b_i on both sides of Eq. (11) and taking average over all nodes, we obtain a closed expression of θ_b^{AI} as

$$\mu\theta_b^{AI} = m_p\beta\{\rho^{AI}[\langle b^2\rangle - (1-\kappa)\theta_{b^2}^A] + \theta_b^{AI}[\langle b\rangle - (1-\kappa)\theta_b^A]\}, \tag{14}$$

where $\theta_{b^2}^A = (1/N)\sum_{j=1}^{N} b_j^2 P_j^A$. Eqs. (13) and (14) can be written in a matrix form as

$$H\begin{bmatrix}\rho^{AI}\\ \theta_b^{AI}\end{bmatrix} = \frac{\mu}{m_p\beta}\begin{bmatrix}\rho^{AI}\\ \theta_b^{AI}\end{bmatrix}, \tag{15}$$

where

$$H = \begin{bmatrix} \langle b\rangle - (1-\kappa)\theta_b^A & 1-(1-\kappa)\rho^A \\ \langle b^2\rangle - (1-\kappa)\theta_{b^2}^A & \langle b\rangle - (1-\kappa)\theta_b^A \end{bmatrix}. \tag{16}$$

When the network system is in the endemic state, we have

$$\begin{bmatrix} \rho^{AI} \\ \theta_b^{AI} \end{bmatrix} \neq \vec{0}.$$

As the disease starts to pervade the network in stationary state, β_c is the minimum value of β that satisfies Eq. (15) [28], making $\mu/(m_p\beta_c)$ be equal to the largest eigenvalue $\Lambda_{max}(H)$ of matrix H, i.e.,

$$\begin{aligned}\Lambda_{max}(H) = &\sqrt{[\langle b^2\rangle - (1-\kappa)\theta_{b^2}^A][1-(1-\kappa)\rho^A]} \\ &+ \langle b\rangle - (1-\kappa)\theta_b^A,\end{aligned} \tag{17}$$

and we thus get

$$\begin{aligned}\beta_c &= \frac{\mu}{m_p\Lambda_{max}(H)} \\ &= \frac{\mu}{m_p}\left\{\sqrt{[\langle b^2\rangle - (1-\kappa)\theta_{b^2}^A][1-(1-\kappa)\rho^A]} + \langle b\rangle - (1-\kappa)\theta_b^A\right\}^{-1}.\end{aligned} \tag{18}$$

It is worth noting that, in Eq. (18), β_c depends explicitly on the network properties of the physical contact layer as described by the quantities m_p and $\langle b\rangle$, $\langle b^2\rangle$, on the information spreading dynamics as quantified by ρ^A, and on the coupling dynamics between the two layers as characterized by the quantities θ_b^A and $\theta_{b^2}^A$.

When information diffusion in the virtual layer is decoupled from the process in the physical layer, the critical value of awareness onset [38] is

$$\lambda_c = \frac{\delta}{m_v(\sqrt{\langle a^2\rangle} + \langle a\rangle)}. \tag{19}$$

Likewise, when the infection process in the physical layer is not coupled with information diffusion in the virtual layer, the values of ρ^A, θ_b^A and $\theta_{b^2}^A$ are all zero. The threshold value in Eq. (18) then becomes

$$\beta_c = \frac{\mu}{m_p(\sqrt{\langle b^2\rangle} + \langle b\rangle)}, \tag{20}$$

which is the epidemic threshold in a single activity driven network. The values (λ_c, β_c) define a metacritical point for epidemic spreading. Only when $\lambda > \lambda_c$ will the onset of the epidemics depend on the dynamics of information diffusion.

The procedure to calculate the quantities ρ^A, θ_b^A and $\theta_{b^2}^A$ can be described, as follows. We first iterate Eqs. (9) and (10) to get P_i^A in the stationary state. We then obtain ρ^A by taking average of P_i^A over all nodes and θ_b^A ($\theta_{b^2}^A$) by multiplying P_i^A and the activity level b_i (b_i^2) of the physical contact network, and taking average of the product over all nodes.

4. Numerical support of theory and mechanisms to inhibit epidemic spreading

To validate our MMC based theoretical analysis, we carry out extensive numerical simulations of spreading dynamics in activity-driven multiplex networks. Given a network, the setting is that initially ($t = 0$), 10% of the nodes are infected, while all others are susceptible. We evolve the iterative interacting dynamics in the virtual and physical layers according to the processes described in Fig. 1. Once the infection density has reached a stationary value, we continue the time evolution for an additional $T = 200$ steps and calculate the average density during this time period so as to reduce the statistical fluctuations to obtain accurate estimates of the epidemic threshold and of the final infection density.

Fig. 2 presents a comparison between theoretical and numerical values of the epidemic threshold for different parameter combinations, where the numerically obtained stationary infection density is color coded and shown as the background. For a fixed parameter set, the dashed curve represents the theoretical threshold value of Eq. (18) as a function of the information transmission rate λ and the markers are the corresponding numerical results, which agree with each other quite well. For $\lambda < \lambda_c$, the epidemic threshold does not depend on the awareness level but, for $\lambda \geq \lambda_c$, the threshold increases with λ. In fact, before the information transmission rate reaches a critical value, information diffusion has little effect on the epidemic. However, if the rate exceeds the critical value, information diffusion in $\mathcal{V}$ can suppress epidemic spreading in the physical contact layer $\mathcal{P}$. We note that previous work [28,29] uncovered the same phenomenon for static multiplex networks.

While the phenomenon that information diffusion is able to suppress epidemic spreading holds for both static and time-varying networks, are there features that are unique to the latter? To answer this question, we note that there are three structural properties that can change the time-varying structure of a multiplex network: the activity exponent γ, the contact capacity m, and the activity correlation c between the two layers. Specifically, the activity exponent characterizes the

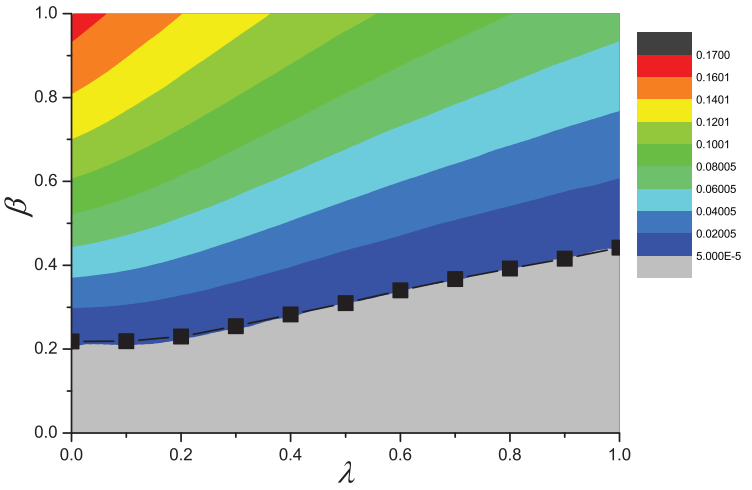

Fig. 2. Comparison between theoretically predicted threshold values and those from Monte Carlo simulations. The color-coded density (ρ_I) values of the infected nodes in the stationary state for different values of λ and β are shown as the background for $\mu = 0.06$ and $\delta = 0.04$. Curve with marker represents the dependence of the critical value β_c^U for the onset of the epidemic on the information transmission rate λ when $\mu = 0.06$ and $\delta = 0.04$. Other parameters are $m_v = m_p = 4$ and $\gamma_v = \gamma_p = 2.1$. The size of each network layer is $N = 10^5$ and the mean degrees of the virtual and physical layers are $\langle k_v \rangle = \langle k_p \rangle = 0.1$.

heterogeneity in the node activity distribution, which leads to heterogeneous time-aggregated networks, where a smaller exponent value indicates a more heterogeneous distribution. Contact capacity is the temporal number of contacts of an average node, and activity correlation quantifies how nodes in the two layer with different activity levels are coupled with each other. In the following, we focus on the role of the three structural properties in suppressing epidemic spreading. A common set of simulation parameters is: $\langle k_v \rangle = \langle k_p \rangle = 0.1$, $\mu = 0.05$, $\delta = 0.05$, and $N = 10^5$ (unless noted otherwise).

4.1. Effect of nodal activity heterogeneity on epidemic spreading

Fig. 3 shows how the epidemic threshold and the final infection density depend on γ_p, the exponent characterizing the heterogeneity of nodal activities in the physical layer. We see that the threshold value increases with γ_p monotonically: a linearly increasing behavior for $\gamma_p <= 3$ and a tendency to get saturated for $\gamma_p > 3$. The final infection density ρ_I versus γ_p exhibits an opposite trend: it decreases with γ_p but the rate of decrease saturates at the turning point about $\gamma_p = 3$. Because a larger value of γ_p means that the nodal activities are less heterogeneous, the results in Fig. 3 indicates that reducing the heterogeneity in the nodal activities in the physical contact layer $\mathcal{P}$ can suppress epidemic spreading. To gain a qualitative understanding of this phenomenon, we decouple the multiplex network and calculate the stationary infection density as a function of the disease transmission rate β in the single layer of physical contact for different values of γ, as shown in the inset of Fig. 3(b). We see that a larger value of the activity exponent leads to a larger threshold value and a smaller value of the final infection density, thereby suppressing epidemic spreading. A heuristic reason is that, when the nodal activities are more heterogeneous, there are nodes in the network that are highly active. These nodes can maintain their activities in consecutive time steps, providing constant driving to the spreading process.

In contrast to the role of nodal activity heterogeneity in the physical layer $\mathcal{P}$, heterogeneity in the nodal activities in the virtual layer $\mathcal{V}$ is in fact beneficial to suppressing epidemic spreading. Specifically, as shown in Fig. 4(a), the epidemic threshold β_c decreases with γ_v for different values of the information transmission rate. The decreasing trend is approximately linear for $\gamma_v \lessapprox 3$ but gradually saturates for $\gamma_v > 3$. A consistent trend occurs for the stationary infection density ρ_I, as shown in Fig. 4(b). The explanation is that, as the value of γ_v is reduced, there are nodes with more heterogeneous activities in $\mathcal{V}$, which serve to accelerate the information diffusion process through a decrease in the information threshold and an increase in the stationary density of the aware nodes. The effect on the physical layer is a larger epidemic threshold and a smaller stationary infection density. As a result, stronger activity heterogeneity in $\mathcal{V}$ can inhibit epidemic spreading in $\mathcal{P}$.

The results of Figs. 3 and 4 thus point at the opposite role played by nodal activity heterogeneity in the physical contact and communication layers: the former promotes but the latter inhibits epidemic spreading. Also, note the emergence of a turning point about $\gamma = 3$, which was also observed in previous studies [43,44]. A possible explanation for the occurrence of the turning point lies in the localization phenomenon in heterogeneous networks [9,12]. Especially, in a network with no correlation, the SIS dynamical transition is governed either by the maximum k-core (if the network is heterogeneous) or by the largest hub (for a homogeneous network). For $\gamma < 3$, varying the value of γ can greatly change the number of nodes with high k-core values. However, for $\gamma > 3$, such a variation has little effect on the maximum degree of the network. These two aspects result in the emergence of the turning point at about $\gamma = 3$.

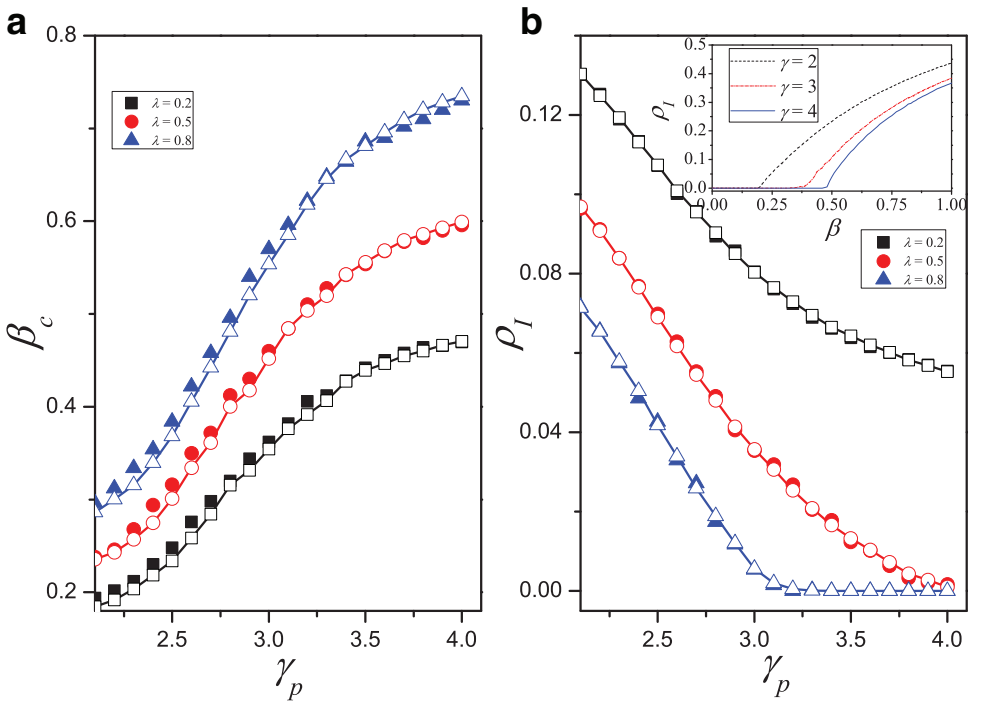

Fig. 3. Effect of activity heterogeneity in physical contact layer on epidemic spreading. Shown are epidemic threshold β_c (a) and the asymptotic density ρ_I of infected nodes (b) versus the activity exponent γ_p for different values of λ, where a larger value of γ_p corresponds to less heterogeneous nodal activities. Open and solid symbols represent the theoretically predicted and simulation results, respectively. In all cases, the epidemic threshold is raised and the final infection density is reduced as the value of γ_p is increased, demonstrating the advantage of making the nodal activities less heterogeneous in suppressing epidemic spreading. Each point is the result of averaging over 100 statistical realizations. Other parameters are $m_v = m_p = 4$ and $\gamma_v = 2.1$. Inset in (b) shows that, for an isolated single physical contact layer, the epidemic threshold value becomes larger as the value of γ is increases, which is consistent with the results in (a) and (b).

4.2. Effect of contact capacity on epidemic spreading

It is convenient to analyze the effect of contact capacity on epidemic spreading separately for the communication and physical layers. We find that increasing the contact capacity m_p in the physical layer has little effect on the epidemic threshold β_c (Fig. 5(a)), but can lead to a decrease in the stationary infection density ρ_I (Fig. 5(b)). The inset of Fig. 5(b) shows the consistent behavior obtained from an isolated, single physical contact layer in terms of the stationary infected density ρ_I versus the disease transmission rate β for different values of m_p, where it can be seen that the epidemic threshold is hardly affected by the contact capacity but the stationary infection density decreases with the capacity. This intriguing phenomenon can be explained theoretically and numerically, as follows.

First, the dynamics in a single physical contact network is investigated. According to the MMC theory, the epidemic threshold of a single physical contact layer is given by

$$\beta_c = \frac{\mu}{m_p(\sqrt{\langle b^2\rangle} + \langle b\rangle)}. \tag{21}$$

For a fixed value of $\langle k_p\rangle$, a change in the contact capacity induces a change in η_p. Using the transform $b_i = \eta_p y_i$, we have

$$\beta_c = \mu/[m_p\eta_p(\sqrt{\langle y^2\rangle} + \langle y\rangle)] = 2\mu/[\langle k_p\rangle(\sqrt{\langle y^2\rangle}/\langle y\rangle + 1)]. \tag{22}$$

Since the quantity $\sqrt{\langle y^2\rangle}/\langle y\rangle$ is constant for a fixed value of the activity exponent γ, the threshold value is unchanged as the contact capacity is varied.

From the perspective of node-based simulations, the time-varying network at a time step is one with a tree structure. For a fixed value of the activity exponent, a larger value of the contact capacity m_p leads to smaller average nodal activities and consequently fewer active nodes in the network. In contrast, a smaller contact capacity is more likely to generate nodes with large activities. The existence of a few active nodes makes little difference when the disease transmission rate is less than the epidemic threshold. However, above the threshold, more active nodes in a network with small contact capacity values make the network more connected, leading to larger epidemic prevalence, as shown in the inset of Fig. 5(b).

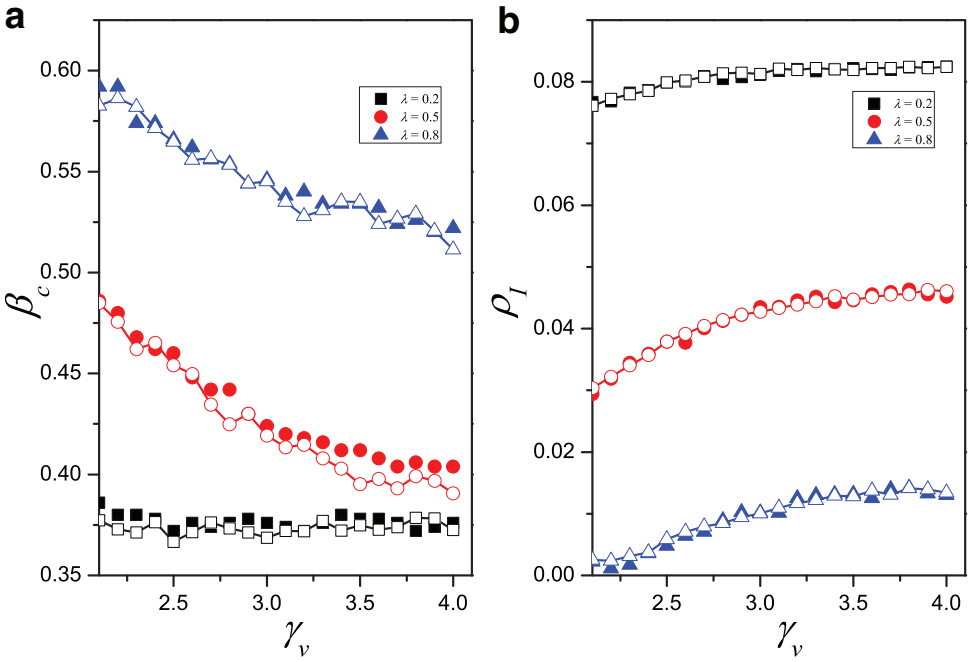

Fig. 4. Effect of activity heterogeneity in the communication layer on epidemic spreading. Shown are epidemic threshold β_c (a) and the final infection density ρ_I (b) versus the activity exponent γ_v in the virtual layer. Each point is the result of averaging over 100 dynamical realizations. Open and solid symbols represent, respectively, results predicted by the MMC theory and from Monte Carlo simulations. Parameters are $m_v = m_p = 4$ and $\gamma_p = 3.1$. As the nodal activities in the virtual communication layer becomes more heterogeneous (corresponding to smaller values of γ_v), the epidemic threshold in the physical layer is enhanced and the final infection density is discounted, indicating the positive role of stronger nodal activity heterogeneity in the virtual layer in suppressing epidemic spreading in the physical layer.

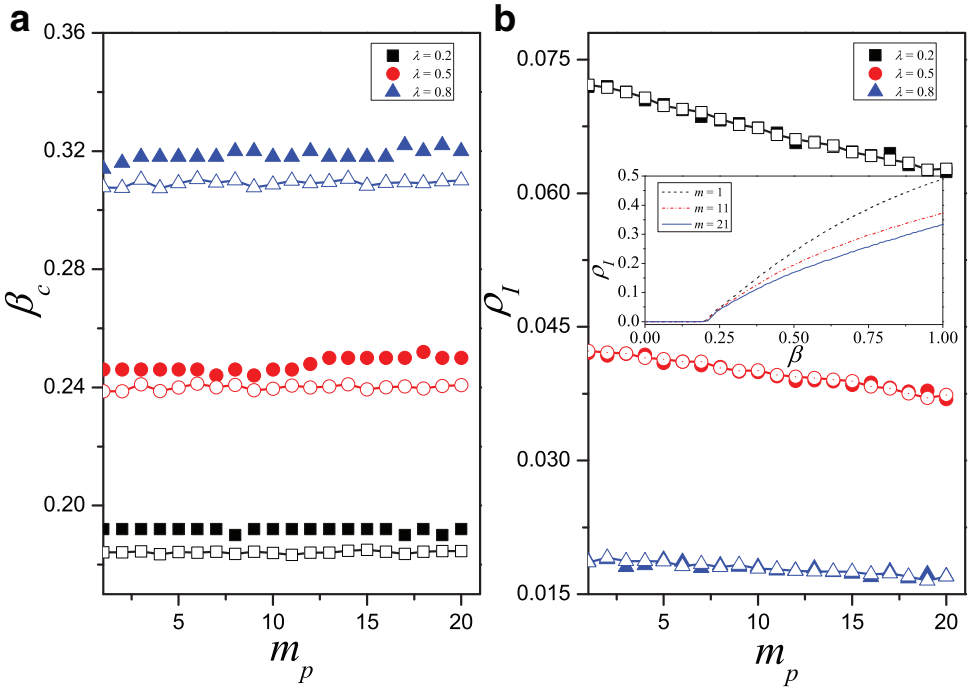

Fig. 5. Effect of varying the contact capacity in the physical layer on epidemic spreading. Shown are the epidemic threshold β_c (a) and the stationary infection density ρ_I (b) versus the contact capacity m_p in $\mathcal{P}$. Open and solid symbols are, respectively, results from MMC prediction and Monte Carlo simulations. Other parameters are $m_v = 1$ and $\gamma_p = \gamma_v = 2.1$. As the capacity is increased, the epidemic threshold hardly changes but the final infection density tends to decrease. The inset in (b) shows the consistent behavior but for an isolated, single physical contact layer.

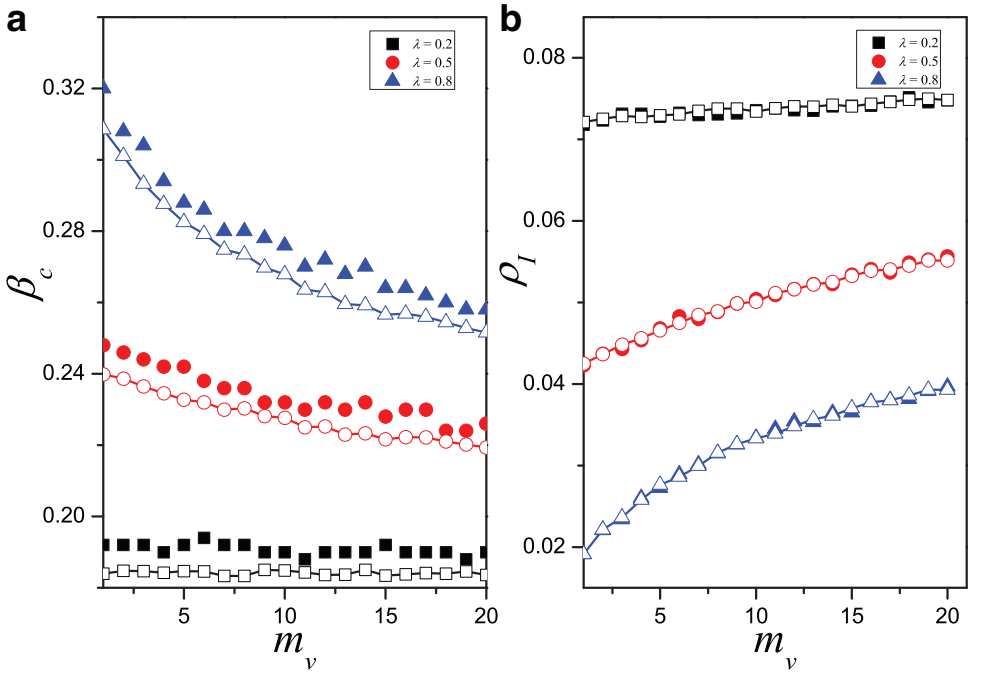

Fig. 6. Effect of varying the contact capacity of the communication layer on epidemic spreading. Shown are the epidemic threshold β_c (a) and the stationary infection density ρ_I (b) versus the contact capacity m_v. Parameters are $m_p = 1$ and $\gamma_p = \gamma_v = 2.1$. Decreasing the value of m_v can enhance the inhibitory effect of information diffusion on spreading in the physical space by increasing the epidemic threshold (a) and reducing the final infection density (b).

Second, the dynamics in multiplex networks is investigated. As shown in Eq. (18),

$$\beta_c = \frac{\mu}{m_p}\left\{\sqrt{[\langle b^2\rangle - (1-\kappa)\theta^A_{b^2}][1-(1-\kappa)\rho^A]} + \langle b\rangle - (1-\kappa)\theta^A_b\right\}^{-1}$$
$$= \frac{2\mu}{\langle k_p\rangle}\left\{\sqrt{[\frac{\langle y^2\rangle}{\langle y\rangle^2} - (1-\kappa)\frac{\theta^A_{y^2}}{\langle y\rangle^2}][1-(1-\kappa)\rho^A]} + 1 - (1-\kappa)\frac{\theta^A_y}{\langle y\rangle}\right\}^{-1}.$$

Once $F_p(y)$, ϵ and parameters in layer V are fixed, $\frac{\langle y^2\rangle}{\langle y\rangle^2}$, $\frac{\theta^A_{y^2}}{\langle y\rangle^2}$, ρ^A and $\frac{\theta^A_y}{\langle y\rangle}$ don't change with m_p statistically. So β_c in multiplex networks doesn't vary with m_p. As the analysis in the single physical contact network above, the stationary infection density ρ_I decreases with the increasing of m_p.

Similarly, in the virtual communication layer $\mathcal{V}$, the contact capacity does not affect the information threshold, but the stationary density of the aware nodes tends to decrease as the contact capacity is reduced, thereby enhancing the inhibitory effect of information diffusion on epidemic spreading through a larger epidemic threshold and smaller epidemic prevalence, as shown in Fig. 6.

Overall, increasing the contact capacity in the physical contact layer can suppress epidemic spreading through a reduction in the epidemic prevalence. Likewise, decreasing the capacity of the communication layer can achieve a similar effect through enhancing the inhibitory role of information diffusion in epidemics.

4.3. Effect of activity correlation on epidemic spreading

In the real world, a certain amount of correlation exists between different contexts in which the individuals play some role. For a multiplex network, this is characterized by the inter-layer degree correlation [24] that can impact the percolation dynamics [8,45,46]. Our focus here is on how the inter-layer activity correlation shapes the inhibitory effect of information spreading on epidemic spreading. To construct a two-layer activity correlated network with a given value of the correlation coefficient c, we use the Spearman rank correlation coefficient [29]. Specifically, for $c > 0$ ($c < 0$), we first generate nodes in a two-layer network with the maximal positive (negative) activity correlation. We then randomly choose $(1 - |c|)N$ pairs of counterpart nodes from different layers, shuffle the activity levels of these nodes in each layer separately, and perform a rematch.

In a network with heterogeneous activities, the less (more) active nodes are in the majority (minority). In a time-varying multiplex network with a negative activity correlation, nodes with large activities in the virtual communication layer are

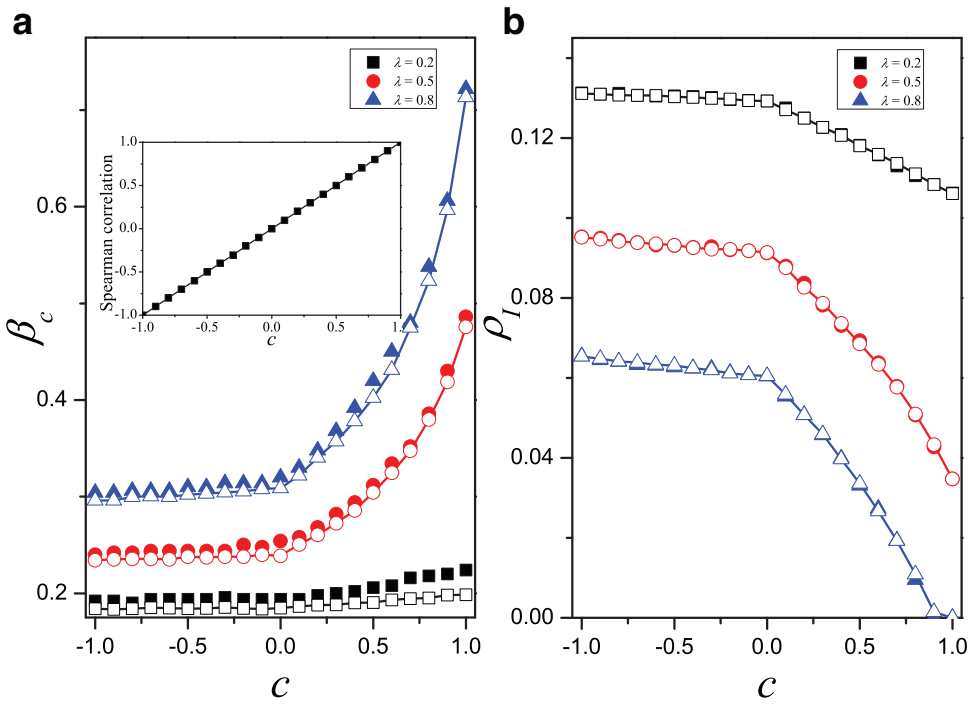

Fig. 7. Effect of inter-layer correlation on epidemic spreading. Shown are epidemic threshold β_c (a) and stationary infection density ρ_I (b) versus the inter-layer activity correlation c. Open and solid symbols are, respectively, theoretical and numerical results. Parameters are $m_v = m_p = 4$ and $\gamma_v = \gamma_p = 2.1$. For negatively correlated networks, varying the value of the correlation coefficient has little effect on both the threshold and the final density. However, the amount of correlation has a dramatic effect on epidemic spreading in positively correlated networks. For such a network, increasing the value of the correlation coefficient can raise the epidemic threshold significantly and reduce the final infection density drastically, suggesting enhancing correlation as an effective control or management strategy to suppress epidemic spreading in time varying multiplex networked systems.

more likely to have small activities in the physical contact layer, and vice versa. In a system with a positive activity correlation, nodes are more likely to have similar activities in both layers. The structural difference among the time-varying multiplex networks with different values of negative correlation is usually small, but positively correlated networks can be structurally quite distinct.

Fig. 7 demonstrates the effect of inter-layer correlation on epidemic spreading. For networks with negative correlation, varying the correlation coefficient has little effect on the epidemic threshold β_c, but for positively correlated networks, the threshold value increases dramatically as the correlation coefficient is increased, as shown in Fig. 7(a). The stationary infection density ρ_I decreases slowly with c for $c < 0$ and but rapidly for $c > 0$, as shown in Fig. 7(b). These behaviors can be explained, as follows. Active nodes in the communication layer are more likely to get information about the epidemic, and active nodes in the physical layer will have more chances to get infected and spread the disease to other nodes. When the multiplex network is negatively correlated, nodes with large activities in the communication layer play a relatively minor role in inhibiting the epidemic. An increase in the correlation coefficient, when it is negative, can enhance the inhibitory effect but not significantly. On the contrary, if the network layers are positively correlated, a slight increase in the number of active nodes in both layers will greatly enhance the inhibitory effect of information diffusion on epidemic dynamics. While the more active nodes are more susceptible to getting infected, they can also obtain information quickly, in turn reducing the chance for them to be infected and to spread the disease.

5. Discussion

To uncover mechanisms and phenomena that can be exploited for suppressing epidemic spreading, taking into account real world constraints, is a problem of significant values to the society. Guided by this general principle and taking into account the fact that social networks in the real world are time varying with a multiplex structure, we have constructed a class of duplex time-varying networks and studied the asymmetrical interplay between epidemic spreading and information diffusion. We have developed a theory by extending the microscopic Markov chain approach to time-varying multiplex networks. The theory enables us to analytically calculate the epidemic threshold and the final infection density. We have conducted extensive Monte Carlo simulations to verify the theoretical predictions. Our theory predicts that the epidemic threshold in the physical contact layer generally depends on the dynamics of information diffusion in the virtual communication layer. A phenomenon that was uncovered previously for static multiplex networks but still holds for time-varying

networks is that, when the rate of information transmission exceeds a threshold, the epidemic threshold in the physical layer can be raised dramatically.

Going beyond the existing work on spreading dynamics in static multiplex networks, we have investigated how the activity properties of the communication and physical layers and their coupling in a time-varying environment affect the epidemic spreading process, with a particular emphasis on the possible inhibitory effect of information diffusion on epidemics. A finding is that nodal activity heterogeneity in physical contact layer tends to facilitate epidemic spreading through reduced epidemic threshold and enhanced prevalence. On the contrary, stronger heterogeneity in the nodal activities in the virtual communication layer can promote inhibitory effect of information diffusion on epidemics. Another finding is that increasing the contact capacity in the physical layer can mitigate the spreading process by producing decreased epidemic prevalence, and a similar effect can be achieved by decreasing the contact capacity in the communication layer. A striking phenomenon has been uncovered when studying the effect of inter-layer activity correlation on epidemic spreading. While a negative correlation plays no apparent role in inhibiting the spreading dynamics, a positive correlation can greatly benefit the inhibitory effect of information diffusion on epidemics. This is because, in a positively correlated multiplex network, nodes with large activities in the physical contact layer are more likely to be associated with a similar level of activities in the virtual communication layer. As a result, active nodes with a high risk of getting infected can quickly obtain the useful information and protect themselves from the disease. Any control or management strategy that can generate a positive correlation in the activities between the two network layers can thus be effective at suppressing epidemic spreading. This result may be useful for informing government policies to prevent large scale epidemic outbreaks.

Our work provides a general framework to study diffusive process in time varying multiplex networks. It is a stepping stone towards further development of co-evolutionary spreading dynamics on realistic multiplex networks and articulation of more effective epidemic control strategies.

Acknowledgments

This work was supported by National Natural Science Foundation of China under Grant Nos. 61803352, 11575041, 61673086, and 11505114 and by the Natural Science Foundation of Shanghai under Grant No. 18ZR1412200). YCL would like to acknowledge support from the Vannevar Bush Faculty Fellowship program sponsored by the Basic Research Office of the Assistant Secretary of Defense for Research and Engineering and funded by the Office of Naval Research through Grant No. N00014-16-1-2828.

References

[1] C. Dye, N. Gay, Modeling the sars epidemic, Science 300 (5627) (2003) 1884–1885.
[2] J.T. Lau, X. Yang, H. Tsui, J.H. Kim, Impacts of sars on health-seeking behaviors in general population in Hong Kong, Preven. Med. 41 (2) (2005) 454–462.
[3] B.J. Park, K.A. Wannemuehler, B.J. Marston, N. Govender, P.G. Pappas, T.M. Chiller, Estimation of the current global burden of cryptococcal meningitis among persons living with HIV/AIDS, Aids 23 (4) (2009) 525–530.
[4] R.J. Garten, C.T. Davis, C.A. Russell, B. Shu, S. Lindstrom, A. Balish, W.M. Sessions, X. Xu, E. Skepner, V. Deyde, et al., Antigenic and genetic characteristics of swine-origin 2009 a (H1N1) influenza viruses circulating in humans, Science 325 (5937) (2009) 197–201.
[5] S. Baize, D. Pannetier, L. Oestereich, T. Rieger, L. Koivogui, N. Magassouba, B. Soropogui, M.S. Sow, S. Keïta, H. De Clerck, et al., Emergence of Zaire Ebola virus disease in Guinea, New Eng. J. Med. 371 (15) (2014) 1418–1425.
[6] R.M. Anderson, R.M. May, Infectious Diseases of Humans: Dynamics and Control, Oxford University Press, 1992.
[7] R. Pastor-Satorras, A. Vespignani, Epidemic spreading in scale-free networks, Phys. Rev. Lett. 86 (14) (2001) 3200.
[8] R. Parshani, S. Carmi, S. Havlin, Epidemic threshold for the susceptible-infectious-susceptible model on random networks, Phys. Rev. Lett. 104 (25) (2010) 258701.
[9] C. Castellano, R. Pastor-Satorras, Thresholds for epidemic spreading in networks, Phys. Rev. Lett. 105 (21) (2010) 218701.
[10] A. Lynch, Thought contagion as abstract evolution, J. Ideas 2 (1) (1991) 3–10.
[11] Z. Tai, T. Sun, Media dependencies in a changing media environment: The case of the 2003 sars epidemic in china, New Media Soc. 9 (6) (2007) 987–1009.
[12] R. Pastor-Satorras, C. Castellano, P. Van Mieghem, A. Vespignani, Epidemic processes in complex networks, Rev. Mod. Phys. 87 (3) (2015) 925.
[13] N. Ferguson, Capturing human behaviour, Nature 446 (7137) (2007) 733.
[14] S. Funk, E. Gilad, C. Watkins, V.A. Jansen, The spread of awareness and its impact on epidemic outbreaks, Proc. Nat. Acad. Sci. (USA) 106 (16) (2009) 6872–6877.
[15] S. Funk, M. Salathé, V.A. Jansen, Modelling the influence of human behaviour on the spread of infectious diseases: a review, J. Roy. Soc. Interface 7 (50) (2010) 1247–1256.
[16] F.D. Sahneh, F.N. Chowdhury, C.M. Scoglio, On the existence of a threshold for preventive behavioral responses to suppress epidemic spreading, Sci. Rep. 2 (2012) 632.
[17] C. Liu, J.-R. Xie, H.-S. Chen, H.-F. Zhang, M. Tang, Interplay between the local information based behavioral responses and the epidemic spreading in complex networks, Chaos 25 (10) (2015) 103111.
[18] A. Lima, M. De Domenico, V. Pejovic, M. Musolesi, Disease containment strategies based on mobility and information dissemination, Sci. Rep. 5 (2015) 10650.
[19] Q. Wu, X. Fu, M. Small, X.-J. Xu, The impact of awareness on epidemic spreading in networks, Chaos 22 (1) (2012) 013101.
[20] F. Bagnoli, P. Lio, L. Sguanci, Risk perception in epidemic modeling, Phys. Rev. E 76 (6) (2007) 061904.
[21] Z. Ruan, M. Tang, Z. Liu, Epidemic spreading with information-driven vaccination, Phys. Rev. E 86 (3) (2012) 036117.
[22] M. Kurant, P. Thiran, Layered complex networks, Phys. Rev. Lett. 96 (13) (2006) 138701.
[23] M. De Domenico, A. Solé-Ribalta, E. Cozzo, M. Kivelä, Y. Moreno, M.A. Porter, S. Gómez, A. Arenas, Mathematical formulation of multilayer networks, Phys. Rev. X 3 (4) (2013) 041022.
[24] M. Kivelä, A. Arenas, M. Barthelemy, J.P. Gleeson, Y. Moreno, M.A. Porter, Multilayer networks, J. Comp. Net. 2 (3) (2014) 203–271.
[25] S. Boccaletti, G. Bianconi, R. Criado, C.I.D. Genio, J. Gómez-Gardeñes, M. Romance, I. Sendiña-Nadal, Z. Wang, M. Zanin, The structure and dynamics of multilayer networks, Phys. Rep. 544 (1) (2014) 1–122.

[26] Q. Wu, T. Hadzibeganovic, Pair quenched mean-field approach to epidemic spreading in multiplex networks, Appl. Math. Model. 60 (2018).
[27] F.D. Sahneh, C.M. Scoglio, Optimal information dissemination in epidemic networks, in: Proceedings of the IEEE 51st Annual Conference on Decision and Control (CDC), IEEE, 2012, pp. 1657–1662.
[28] C. Granell, S. Gómez, A. Arenas, Dynamical interplay between awareness and epidemic spreading in multiplex networks, Phys. Rev. Lett. 111 (12) (2013) 128701.
[29] W. Wang, M. Tang, H. Yang, Y. Do, Y.-C. Lai, G. Lee, Asymmetrically interacting spreading dynamics on complex layered networks, Sci. Rep. 4 (2014) 5097.
[30] C. Granell, S. Gómez, A. Arenas, Competing spreading processes on multiplex networks: awareness and epidemics, Phys. Rev. E 90 (1) (2014) 012808.
[31] Q.-H. Liu, W. Wang, M. Tang, H.-F. Zhang, Impacts of complex behavioral responses on asymmetric interacting spreading dynamics in multiplex networks, Sci. Rep. 6 (2016) 25617.
[32] E. Massaro, F. Bagnoli, Epidemic spreading and risk perception in multiplex networks: a self-organized percolation method, Phys. Rev. E 90 (5) (2014) 052817.
[33] T. Gross, C.J.D. D'Lima, B. Blasius, Epidemic dynamics on an adaptive network, Phys. Rev. Lett. 96 (20) (2006) 208701.
[34] H. Yang, M. Tang, H.-F. Zhang, Efficient community-based control strategies in adaptive networks, New J. Phys. 14 (12) (2012) 123017.
[35] H. Yang, M. Tang, T. Gross, Large epidemic thresholds emerge in heterogeneous networks of heterogeneous nodes, Sci. Rep. 5 (2015) 13122.
[36] H. Yang, T. Rogers, T. Gross, Network inoculation: heteroclinics and phase transitions in an epidemic model, Chaos 26 (8) (2016) 083116.
[37] P. Holme, J. Saramäki, Temporal networks, Phys. Rep. 519 (3) (2012) 97–125.
[38] N. Perra, B. Gonçalves, R. Pastor-Satorras, A. Vespignani, Activity driven modeling of time varying networks, Sci. Rep. 2 (2012) 469.
[39] E. Valdano, L. Ferreri, C. Poletto, V. Colizza, Analytical computation of the epidemic threshold on temporal networks, Phys. Rev. X 5 (2) (2015) 021005.
[40] M. Starnini, A. Baronchelli, R. Pastor-Satorras, Modeling human dynamics of face-to-face interaction networks, Phys. Rev. Lett. 110 (16) (2013) 168701.
[41] M. Génois, C.L. Vestergaard, C. Cattuto, A. Barrat, Compensating for population sampling in simulations of epidemic spread on temporal contact networks, Nat. Commun. 6 (2015) 8860.
[42] A. Moinet, M. Starnini, R. Pastor-Satorras, Burstiness and aging in social temporal networks, Phys. Rev. Lett. 114 (10) (2015) 108701.
[43] W. Wang, M. Tang, H.-F. Zhang, H. Gao, Y. Do, Z.-H. Liu, Epidemic spreading on complex networks with general degree and weight distributions, Phys. Rev. E 90 (4) (2014) 042803.
[44] Y.-X. Zhu, W. Wang, M. Tang, Y.-Y. Ahn, Social contagions on weighted networks, Phys. Rev. E 96 (1) (2017) 012306.
[45] K.-M. Lee, J.Y. Kim, W.-K. Cho, K.-I. Goh, I. Kim, Correlated multiplexity and connectivity of multiplex random networks, New J. Phys. 14 (3) (2012) 033027.
[46] W. Wang, Q.-H. Liu, S.-M. Cai, M. Tang, L.A. Braunstein, H.E. Stanley, Suppressing disease spreading by using information diffusion on multiplex networks, Sci. Rep. 6 (2016) 29259.